Noechel, U.; Reddy, C.S.; Uttamchand, N.K.; Kratz, K.; Behl, M.; Lendlein, A.:

Shape-memory properties of hydrogels having a poly (Epsilon-caprolactone) crosslinker and switching segment in an aqueous environment

In: European Polymer Journal (2013) Elsevier

DOI: 10.1016/j.eurpolymj.2013.01.022

Shape-Memory Properties of Hydrogels Having a Poly(ε-caprolactone) Crosslinker and Switching Segment in an Aqueous Environment

Ulrich Nöchel[1*], Chaganti Srinivasa Reddy[1,2*], Narendra Kumar Uttamchand[1], Karl Kratz[1], Marc Behl[1,2] and Andreas Lendlein[1,2,#]

** Authors contributed equally to this work*
[#] Corresponding author: Prof. Andreas Lendlein
[1] Institute of Biomaterial Science and Berlin-Brandenburg Center for Regenerative Therapies, Helmholtz-Zentrum Geesthacht, Kantstr. 55, 14513 Teltow, Germany
[2] Tianjin University-Helmholtz-Zentrum Geesthacht, Joint Laboratory for Biomaterials and Regenerative Medicine, Weijin Road 92, Tianjin 300072, China
E-mail: andreas.lendlein@hzg.de
Phone: +49 (0)3328 352-450
Fax: +49 (0)3328 352-452

Abstract

Multiphase copolymer networks are of great relevance as their thermal and mechanical as well as shape-memory properties can be adjusted by the variation of the composition and crosslink density. In this context recently grafted copolymer networks (named CLEG), prepared by thermal free-radical polymerization with different ratios of the hydrophobic telechelic crosslinker poly(ε-caprolactone) diisocyanoethyl methacrylate (PCLDIMA, $T_{m,PCL}$ = 55 °C) and hydrophilic poly(ethylene glycol) monomethyl ether monomethacrylate (PEGMA, $T_{m,PEG}$ = 38 °C) as co-monomer, were introduced, which additionally allow the alteration of the overall elastic properties via controlled water uptake.

Here we study the thermomechanical properties as well as the shape-memory behavior of a series of CLEG copolymer networks in an aqueous environment. The mechanical properties of the networks at 25 °C in aqueous environment were found to increase from 4 MPa to 77 MPa with increasing crosslink density. The shape-memory properties of the copolymer networks were examined in an aqueous environment by both bending as well as uniaxial elongation experiments. Excellent dual-shape properties with high shape fixity ratios around R_f = 79-100% and shape recovery ratios in the range of R_r = 59% to R_r = 100% were obtained for copolymers with a PCLDIMA weight fraction ≥ 50 wt% in the starting composition. The swelling of CLEG in H_2O resulted in a reduction of the switching temperature. Furthermore the structural changes during programming of CLEG were assessed *in situ* by small and wide angle X-ray scattering (SAXS, WAXS) experiments, which confirmed that the overall degree of crystallinity as well as the orientation of the crystalline domains controlled the dual-shape performance. We have found that an appropriate switching segment should result in a degree

of crystallinity higher than 10–20% to enable high strain fixity ratios. Furthermore, hydrogels having dual shape-memory capability could be created by using semi-crystalline crosslinker simultaneously acting as the switching segment.

Keywords:
Shape-memory polymer, hydrogel, polymer network, stimuli-sensitivity

1. Introduction

Shape-memory polymers (SMPs) have the ability to recover their original/permanent shape upon exposure to an external stimulus, after being deformed and fixed into a temporary shape before [1]. SMPs can be applied as actuators, sensors, and for biomedical applications [2, 3]. The most prominent class of SMPs are thermo-sensitive polymers, which exhibit a dual-shape effect when the switching temperature (T_{sw}) is exceeded. While the permanent shape of dual-shape materials is determined by netpoints, the temporary shape is fixed by reversible crosslinks related to a thermal transition (T_{trans}), which can be a glass (T_g) or melting transition (T_m) [4]. T_{trans} of a SMP is typically adjusted by the polymer molecular structure, e.g. the chemical composition or/and the molecular weight of the switching segment. Alternatively, T_{trans} and in this way T_{sw} can be influenced e.g. by the humidity where water molecules act as plasticizers and lower the T_g of the switching domains [5-8]. Additionally the uptake of water into an amorphous polymer matrix induces softening of the material.

Besides solely polymeric materials, a shape-memory capability was also reported for hydrogels thereof, which are of particular interest for biomedical applications, as these soft materials exhibit elastic properties comparable with biological tissues [9]. Such dual-shape hydrogels are typically semi-crystalline polymer networks containing water swellable moieties [9-13] and therefore exhibit shape-memory capability in an aqueous environment. These dual shape hydrogels were composed of water swellable main chains and crystallizable side chains, and the mechanical properties were controlled by the weight fraction of crystallizable side chains. In order to differentiate hydrogels from swollen polymers, a minimum water uptake of 10–20 wt% should be provided [14]. Recently multiphase copolymer networks composed of two crystallizable switching segments, poly(ε-caprolactone) diisocyanatoethyl methacrylate (PCLDIMA) acting as crosslinker and grafted poly(ethylene glycol) monomethyl ether monomethacrylate (PEGMA), named CLEG have been reported [15-17], having dual- and triple-shape-memory capability in the dry state. As

one phase was hydrophilic PEG, we recently reported the influence of water uptake on the thermal properties and degree of crystallinity of CLEG in an aqueous environment [18]. These hydrogels exhibited an elevated degree of swelling in water up to 263±1%. It was observed that all PEG crystalline domains disappeared when the copolymer was swollen in water, whereas the crystalline PCL domains remained. This prompted us to investigate whether CLEG can exhibit a dual-shape-memory effect in an aqueous environment, which might be controlled by the composition of the copolymer (e.g. the PCLDIMA content).

In this study a series of CLEG copolymer networks having a PCLDIMA content in the range from 30 wt% to 70 wt% of in the starting mixture was synthesized, and the resulting copolymer networks were exposed to an aqueous environment for 24 h prior to the investigation of their thermomechanical as well as shape-memory properties.

The thermomechanical properties of such equilibrated grafted multiphase copolymer networks were explored by means of differential scanning calorimetry (DSC), dynamic mechanical thermal analysis (DMTA) and uniaxial tensile tests. In addition, the dual-shape properties of CLEG in an aqueous environment were determined by bending and uniaxial elongation experiments. In case of uniaxial stretching experiments, *in situ* small and wide angle X-ray scattering (SAXS, WAXS) experiments were conducted on CLEG in aqueous environment to investigate the nanostructural parameters, which influence the strain fixity and recovery ratios of the dual-shape effect.

2. Experimental details

2.1 *Synthesis*

The copolymer networks were prepared as reported earlier [15, 19]. The different compositions were obtained by adjusting the ratio of PCLDIMA (M_n = 8300 g·mol^{-1}, $T_{m,PCL}$ = 55 °C) to PEGMA (M_n = 1000 g·mol^{-1}, $T_{m,PEG}$ = 38 °C) in the starting reaction mixture. For the preparation of CLEG50, 3.5 g of PCLIDMA and 3.5 g of PEGMA were heated to 80 °C under stirring and held under vacuum for 30 min to remove volatile components. By adding 10.6 mg benzyl peroxide the radical polymerization was initiated. Immediately the reaction mixture was poured between two glass plates adjusted to 1 mm height by a Teflon® spacer and kept at 80 °C for 24 h.

For evaluation of the crosslinking reaction, the copolymer networks were extracted with chloroform. The gel content *G*, which was calculated according to Eq. (1), as quotient of the mass of the extracted and dried films (m_d) to the mass of the original crude sample (m_c).

$$G = \frac{m_d}{m_c} \cdot 100 \qquad (1)$$

2.2 ***Swelling capability in aqueous environment***

The volumetric degree of swelling in water (Q) was calculated using Eq. (2), here m_s and m_c represent the swollen and dry weights of the networks and the specific densities of the solvent (ρ_s) and the polymer network (ρ_m), as determined with an Ultra Pycnometer (Quantachrome, Odelzhausen, Germany) at 25 °C using a measurement cell with a calibration volume of 1.0725 cm^3.

$$Q = \left[1 + \frac{\rho_m}{\rho_s} \cdot \left(\frac{m_s}{m_c} - 1 \right) \right] \cdot 100 \qquad (2)$$

2.3 ***Differential scanning calorimetry (DSC)***

DSC experiments were conducted on a Netzsch DSC 204 Phoenix (Selb, Germany) at heating and cooling rates of 10 $K \cdot min^{-1}$ in sealed aluminum pans. The networks in aqueous environment were investigated in the temperature range from -100 °C to 70 °C, first cooled from room temperature to -100 °C, then heated to 70 °C and again cooled to -100 °C and finally reheated to 70 °C. The melting temperatures and enthalpies were determined from second heating run.

2.4 ***Dynamic mechanical analysis at varied temperature (DMTA)***

DMTA measurements were performed on a Gabo Eplexor 25 N (Ahlden, Germany) using standard test specimen (ISO 527-2/1BB) punched from polymer network films and swollen overnight in water. All experiments were performed in temperature sweep mode with constant heating rate of 1 $K \cdot min^{-1}$ in water. The oscillation frequency was 10 Hz. The samples were investigated in a thermochamber in a temperature interval from -10 °C to 90 °C. The actual temperature of the sample in water was measured during the experiment by placing a thermocouple in the water near the sample.

2.5 ***X-ray scattering (WAXS and SAXS)***

X-ray scattering of polymer networks under aqueous environment was conducted by enclosing the samples between thin polycarbonate X-Ray films preventing the evaporation of water.

WAXS measurements were performed on an X-ray diffractometer D8 Discover with a two-dimensional Hi-Star detector (105 µm pixel size) from Bruker AXS (Karlruhe, Germany). The X-ray generator was operated at a voltage of 40 kV and a current of 40 mA on a copper anode. A graphite monochromator produced Cu-K_α radiation (0.154 nm wavelength) and a 3 pinhole collimator with an opening of 0.8 mm was used. The distance between sample and detector was 150 mm, calibrated with Corundum standard.

Integration of intensity versus scattering angle 2θ led into one-dimensional curves for analysis, which were decomposed into peaks from crystalline, amorphous and water phases. The crystallinity index (x_c) was determined from the integrated areas of crystalline and amorphous peaks using Eq. (3). Crystal sizes were determined with the Scherrer equation [20] considering k = 0.9.

$$x_c = \frac{A_{cryst}}{A_{cryst} + A_{amorph}} \cdot 100 \qquad (3)$$

SAXS measurements were conducted on a small-angle diffractometer Nanostar (Bruker AXS, Karlruhe, Germany) equipped with a two dimensional VANTEC-2000 detector (68 µm pixel size) employing a wavelength of 0.154 nm. The distance sample to detector was 1070 mm calibrated with silver behenate standard; the beam size was 400 µm. The 2D-scattered patterns, of intensity versus scattering vector $\mathbf{s} = (s_1,s_2,s_3)$ being $|s| = (2/\lambda)\sin\theta$ [21], were integrated after background subtraction over a 10° wide chi range along both the $s_{1,2}$ and s_3 axis (parallel and perpendicular to the drawing direction) leading into a one-dimensional curve I versus $s_{1,2}$ or s_3. Long periods were determined from the position of the peak maxima after Lorentz correction ($I(s) \rightarrow s^2I(s)$) as $L = 1/s_L$.

2.6 *Dual-shape experiments in aqueous environment*

2.6.1 Bending experiments

The dual-shape properties of CLEG hydrogels were determined by both bending and uniaxial stretching experiments in aqueous environment. Films were cut into standard samples (ISO 527-2/1BB) and swollen for 24 h to equilibrium in distilled water.

During the programming for bending experiments under water the straight sample with angle of $\theta_p = 0°$ was heated to $T_{high} = 70$ °C and deformed by bending to an angle of $\theta_i = 180°$. The deformed sample was cooled at 5 K·min^{-1} to $T_{low} = 5$ °C while the external strain was kept constant and equilibrated for 30 min. Finally, the external strain constraint was removed and the bending angle of temporary shape θ_t was obtained (c.f. **Fig. 1**). The recovery of the permanent shape was initiated by heating the programmed samples in aqueous

environment from 10 °C to 55 °C at a rate of 5 K·min^{-1}. The change in bending angle was documented with a digital camera (Canon, PowerShot A460) and after the completion of the recovery process, the recovered angle θ_f was determined. The dual-shape properties were quantified by calculating the shape fixity ratio (R_f) from Eq. (4) and the shape recovery ratio (R_r) from Eq. (5).

$$R_f = \frac{\theta_t - \theta_p}{\theta_i - \theta_p} \times 100 \qquad (4)$$

$$R_r = \frac{\theta_t - \theta_p}{\theta_t - \theta_f} \times 100 \qquad (5)$$

2.6.2 Uniaxial stretching experiment

Uniaxial stretching experiments in aqueous environment were conducted with a Zwicki Z2.5 (Zwick GmbH, Ulm, Germany) equipped with a 20 N load cell and on samples immersed in a water thermal tank, where the temperature was controlled with an Ecoline Star Edition RE306 (Lauda, Königshofen, Germany). The samples were strained at 2 mm·min^{-1}. The actual temperature of the sample was measured by a Voltcraft multi-thermometer DT-300 positioned near the sample.

CLEG hydrogel was deformed to an elongation ε_m = 50% at T_{high} = 70 °C for samples having 40 wt% and above of PCL segment, where the strain was kept constant for 5 min to allow relaxation. Then the sample was cooled at 5 K·min^{-1} to T_{low} = 5 °C under constant-strain and equilibrated for 10 min. Finally, the stress was removed and the elongation of the sample in the temporary shape $\varepsilon_u(N)$ was obtained. The recovery of the sample under stress controlled conditions was induced by heating the programmed sample to T_{high} with a heating rate of 2 K·min^{-1}. After the completion of the recovery process $\varepsilon_p(N)$ was determined, as well as T_{sw}, which was obtained as inflection point in the strain-temperature recovery curve.

The extent to which the deformation (ε_m) applied during shape-memory creation procedure (SMCP) could be fixed, was quantified by the shape fixity ratio R_f and calculated according to Eq. (6). Similarly, the ability of the material to recover its original shape was quantified by the shape recovery ratio R_r using Eq. (7).

$$R_f = \frac{\varepsilon_u(N) - \varepsilon_p(N)}{\varepsilon_m(N) - \varepsilon_p} \times 100 \qquad (6)$$

$$R_r = \frac{\varepsilon_u(N) - \varepsilon_p(N)}{\varepsilon_u(N) - \varepsilon_p} \times 100 \qquad (7)$$

Additionally, the obtained stress-strain data were analyzed by Mooney-Rivlin equations for calculation of network crosslink density (Eq. (8) for dry systems, Eq. (9) for swollen systems, and Eq. (10)) [22-24]:

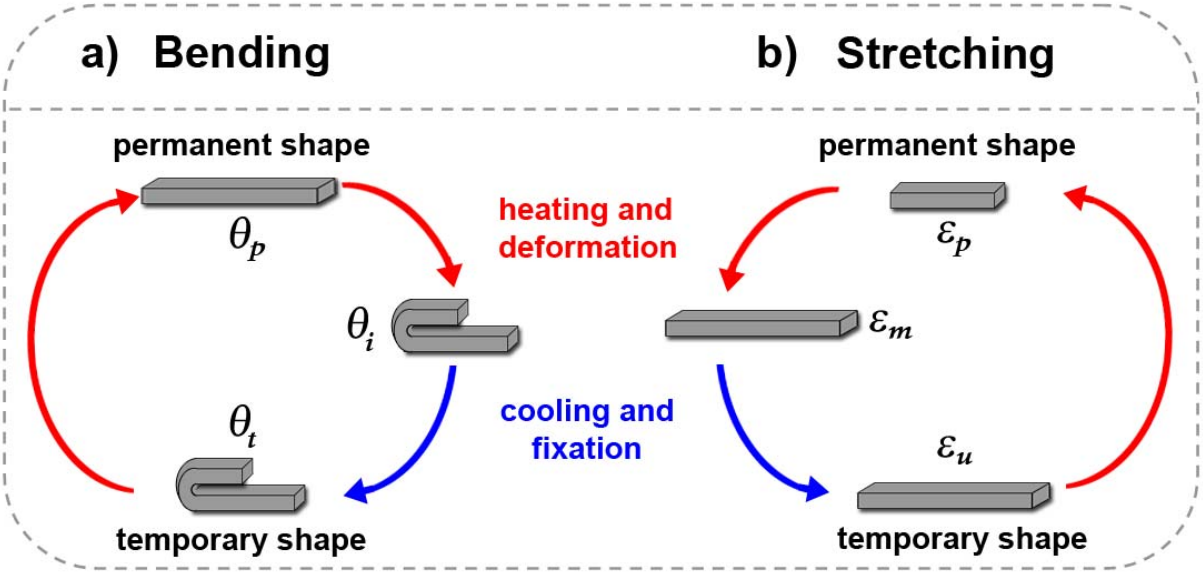

Figure 1: Schematic illustration of the dual-shape programming and recovery for bending (a) and stretching (b) experiments. Both experiments were conducted on CLEG hydrogels in an aqueous environment.

$$\frac{\sigma_n}{\lambda - \lambda^{-2}} = 2C_1 + \frac{2C_2}{\lambda} \qquad (8)$$

$$\frac{\sigma_n \cdot v_p^{1/3}}{\lambda - \lambda^{-2}} = 2C_1 + \frac{2C_2}{\lambda} \qquad (9)$$

$$\nu_c = \frac{2C_1 + 2C_2}{RT} \qquad (10)$$

where σ_n is the applied tensile stress, λ is the strain rate, ν_p is the volume fraction of the polymer in the swollen system, $2C_1$ and $2C_2$ are the Mooney-Rivlin constants, R is the gas constant (8.314 $J \cdot K^{-1} \cdot mol^{-1}$) and T is the absolute temperature and ν_c is the crosslink density.

3. Results and discussion

3.1 *Composition and morphology*

Copolymer networks having 30-70 wt% of PCLDIMA in the starting reaction mixture were synthesized by thermally initiated free-radical polymerization. Samples were denoted

according to the wt% of PCLDIMA (c.f. **Table 1**). The yield of the crosslinking reaction as determined by the gel content (*G*) [25] was above 96% for all CLEG samples indicating an almost complete crosslinking reaction independent from the composition as reported earlier [18].

Table 1: Swelling behavior, thermal and mechanical properties and crosslink densities of CLEG polymer network in dry and aqueous environment.

Q (25 °C) [b]	$T_{m,PCL}$ [c]	ΔH_m [c]	E (25 °C) [d]	E (dry) [d]	ε_B (25 °C) [d]	ε_B (dry) [d]	E (70 °C) [d]	σ_{max} (70 °C) [d]	υ_c (70 °C) [e]
[%]	[°C]	[J·g^{-1}]	[MPa]	[MPa]	[%]	[%]	[MPa]	[MPa]	[mol·m^{-3}]
263±1	40	5±2	4±3	12±1	21±7	78±6	0.71±0.05	0.14±0.05	82±4
208±3	41	10±2	9±2	25±1	40±20	170±30	0.85±0.09	0.20±0.07	103±9
172±1	42	19±2	21±2	44±1	53±7	270±30	1.1±0.2	0.37±0.01	136±10
148±2	44	22±2	38±2	71±4	60±3	300±50	1.1±0.2	0.40±0.02	140±10
127±2	46	29±2	77±9	104±3	50±10	350±30	1.56±0.04	0.49±0.02	152±10

D the two-digit number gives the weight content of PCLDIMA in wt% in the starting reaction mixture. [b] Volumetric degree of swelling determined by gravimetric relation. [c] Melting t as determined by DSC. [d] Young's Modulus (E), elongation at break (ε_B) and maximum stress (σ_{max}) determined by tensile tests at temperatures as indicated. Data of dry polymer netwo mparison. [e] Crosslink densities as determined by Mooney-Rivlin analysis.

Dry polymer networks were swollen in water until equilibrium (e.g. constant weight). A scheme of CLEG network formation is shown in **Fig. 2**. The volumetric degree of swelling in water (Q) at room temperature decreased from 263 ± 1% to 127 ± 2% with increasing in PCL wt%, which was attributed to the hydrophobic character of the PCL segment. In contrast Q increased exponentially in CLEG hydrogels with increasing PEG content, which was related to the storage of free water at higher PEG wt% (i.e. for CLEG40 and CLEG30). Lower PEG wt%, as for CLEG70, would allow only bound water to be incorporated to the PEG segments [26]. Q at T_{high} = 70 °C decreased from 238 ± 1% to 129 ± 2% with increasing in PCL wt% as related to the hydrophobic character of the PCL, slightly lower Q at 70 °C than at 25 °C for CLEG having ≤ 50 wt% of PCL segment was attributed to the higher mobility of the PCL phase at $T > T_{m,PCL}$ and the decreased density of H_2O at 70 °C, resulting in a slightly lowered overall water uptake.

3.2 *Thermal and mechanical properties*

Thermal properties of the CLEG hydrogels in aqueous environment were investigated by DSC and DMTA. A melting transition temperature related to crystalline PCL domains ($T_{m,PCL}$) was observed in the range between 40 °C and 46 °C.

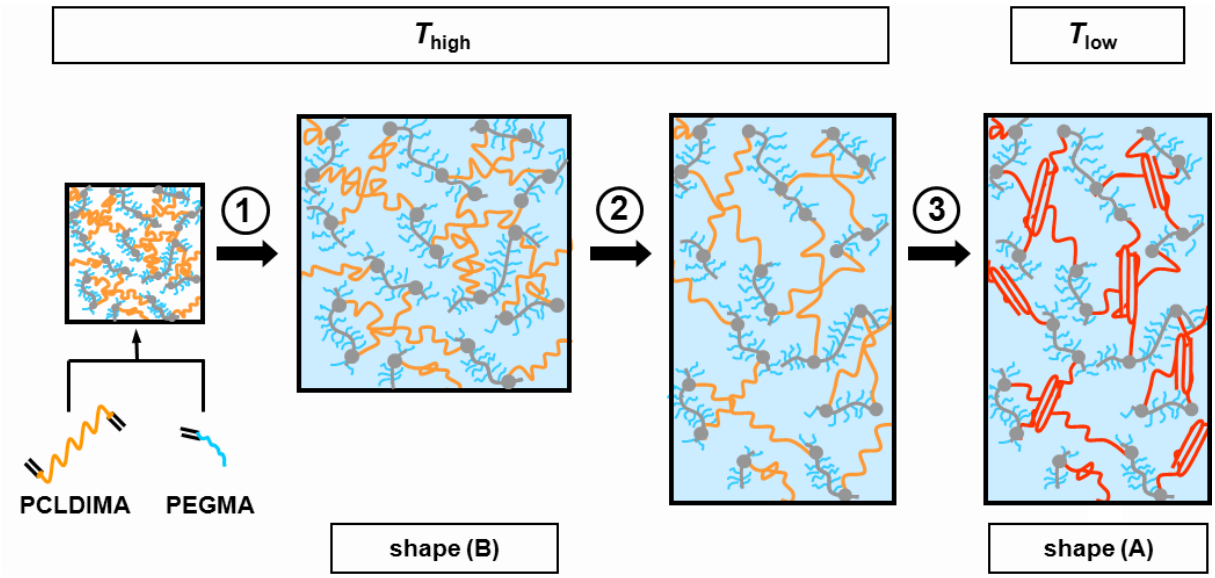

Figure 2: Schematic representation of the molecular mechanism during dual-shape creation procedure of CLEG in aqueous environment. The different colors symbolize the different domains of the copolymer. Orange: amorphous PCL chain segments, red: crystalline PCL chain segments, light blue: amorphous PEG chain segments, grey: amorphous poly(methacrylate) chain segments, transparent blue background: water. ① represents swelling until equilibrium of CLEG polymer networks at T_{high}, ② represents the deformation step at T_{high}, and ③ represents the fixation of the temporary shape after crystallization of PCL chain segments at T_{low}.

The $T_{m,PCL}$ increased with increasing PCL content in the starting reaction mixture (see **Table 1**), which was attributed to an improved crystallization of the PCL chain segments in the CLEG matrix. An increased wt% of PCL in CLEG under aqueous environment resulted in larger hydrophobic regions and permitted the formation of larger crystals, consequently $T_{m,PCL}$ was increased. As compared to dry CLEG the T_m of PCL was lowered, being 50 °C in the absence of an aqueous environment [18], which was attributed to the increased volume of the swollen PEG phase, imposing a certain level of mechanical stress on the PCL phase resulting in a slightly hindered crystallization of the PCL, where smaller crystals resulted in lower $T_{m,PCL}$. The total amount of crystallites in CLEG hydrogels as reflected by the melting enthalpy (ΔH_m) increased with increasing PCL content from 5 $J \cdot g^{-1}$ for CLEG30 to 29 $J \cdot g^{-1}$ for CLEG70, which was related to the higher amount of PCL crystalline fraction. This observation is complemented by WAXS experiments.

The glass transition temperatures of dry CLEG and CLEG hydrogels were found at T < -60 °C as described in [18] and did not contribute to the temperature range of the present study (i.e. 5-70 °C).

The mechanical properties during DMTA analysis of CLEG and CLEG hydrogels are shown in **Fig. 3a** and **b** respectively. A plateau at lower temperatures can be observed followed by a drop of the storage modulus close to the T_m, leading into a second plateau at high temperatures, which is characteristic for polymer networks as the elasticity is provided by the covalent crosslinks. We observed that the storage modulus at room temperature of the dry CLEG was independent of the chemical composition, having values around 400 MPa. This was related to the existence of two crystalline fractions (PCL and PEG) contributing to the elasticity and led into a relative constant degree of crystallinity as reported previously [18]. For CLEG under aqueous environment this behavior was different, showing the storage modulus a dependency to the chemical composition. At room temperature E' increased from 7 MPa for CLEG30 to 100 MPa for CLEG70 with increasing PCL wt%, which was attributed to the increased crystallinity as observed by DSC and WAXS [18]. The swollen PEG segment was unable to crystallize in aqueous environment and could not contribute to the elasticity of the polymer network.

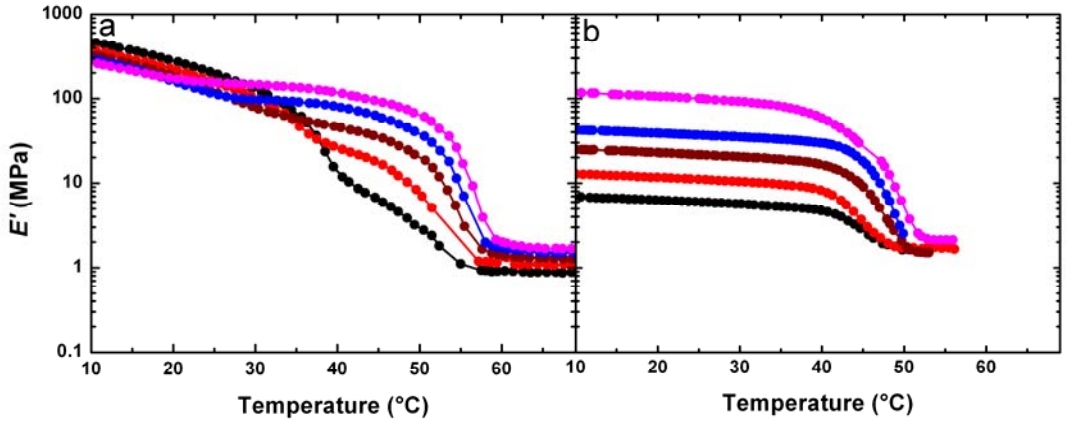

Figure 3: DMTA curves (storage modulus *E´* versus temperature) of: CLEG30 (black), CLEG40 (red), CLEG50 (brown), CLEG60 (blue), and CLEG70 (magenta) in (a) dry state (b) in an aqueous environment.

The temperature, at which the storage modulus decreased abruptly, corresponded to the PCL crystal melting temperature ($T_{m,PCL}$) of the CLEG hydrogel as determined by DSC measurement. The range where *E'* dropped due to the melting of PCL crystallites, was found to be narrowed for CLEG hydrogels as compared to the dry CLEG, which we attributed to the existence of only one melting transition in CLEG under aqueous environment. In contrast, dry systems had two melting transitions (PEG and PCL), which resulted in a broad mechanical transition. At high temperatures, once *E*' decreased to a plateau, the plateau had a slightly higher *E*' for the CLEG in aqueous medium. This was related to the effect of the primary bound water of the PEG side chains, which could lead into a stiffening of the hydrogel and consequently exhibit an increased storage modulus [26].

Mechanical testing of CLEG networks was performed under uniaxial stress in both dry conditions and aqueous environment; results are shown in **Table 1**. At room temperature the elastic modulus was higher for CLEG with the same composition than for the corresponding hydrogels, which was also observed during DMTA and could be related to the additional crystalline PEG fraction in the dry CLEG. For CLEG hydrogels *E* increased from 4 MPa for CLEG30 to 77 MPa for CLEG70, which was attributed to the increased crystallinity provided by the rising PCL wt%. At T = 70 °C CLEG hydrogel had a significantly lower *E* as the PCL was amorphous and only chemical crosslinks contributed to the elasticity. *E* increased from 0.14 MPa for CLEG30 to 1.56 MPa for CLEG70 with increasing PCL wt%, related to the higher crosslink density. This observation was confirmed by Mooney-Rivlin analysis of dry CLEG networks and swollen networks under aqueous environment at $T > T_m$ (i.e. 70 °C) as shown in **Table 1**. The dry polymer networks had an increased crosslink density (ν_c) with increasing PCL wt%, rising from ν_c = 65 mol·m^{-3} for CLEG30 to ν_c = 160 mol·m^{-3} for

CLEG70. CLEG in aqueous environment exhibited a slightly higher ν_c for CLEG30, CLEG40, and CLEG50 as compared to the dry systems. In the dry state at T = 70 °C only chemical crosslinks and chain entanglements are contributing to the crosslink density. Once the sample is swollen in water, there is bound water surrounding the hydrophilic PEG-side-chain. This leads into an increase of the volume of the hydrophilic phase, which leads into orientation of the main chain (PCL). This strain is reflected in the mechanical properties, as can be observed in an increased storage modulus at T = 70 °C for swollen CLEG (**Fig. 3**). Similar findings have been previously reported for highly swollen polymer networks [26]. This increased mechanical stiffness could contribute to the increased ν_c-value, as it was obtained from tensile testing. Nonetheless, this effect is only observed at PEG-contents higher than 40 wt%.

3.3 *Dual-shape properties in aqueous environment*

The dual-shape properties of CLEG hydrogels were determined by both uniaxial tensile tests and bending experiments, where the programming and the recovery were conducted in aqueous environment. A one-step deformation SMPC was applied for generating the temporary shape, followed by a recovery module, where the permanent shape was recovered. A detailed description is given in the experimental section and a schematic illustration is given in **Fig. 1**, whereby the molecular mechanism is displayed in **Fig. 2**.

The shape-memory characteristics, e.g. R_f and R_r of CLEG, achieved under aqueous environment are presented in **Table 2**. Here a strong dependence of R_f on the composition (PCL-content) becomes apparent, whereby the R_f – values increased from 42% ± 2% (bending test) and 33% ± 1% (tensile test) for CLEG30 to 100% ± 2% for CLEG60 and CLEG70. We attributed this observation to the overall crystalline fraction (PCL) remaining in the CLEG hydrogels. As observed by WAXS, CLEGs having R_f = 100%, exhibited a higher degree of orientation (c.f. **Fig. 6c**) as well as the highest melting enthalpy (**Table 1**). Thus, CLEG60 and CLEG70 had a sufficient quantity of crystalline PCL fraction to generate oriented crystals after crystallization, which lead into a higher shape fixing capability. CLEG hydrogels with lower crystallinity exhibiting lower R_f could generate only a small fraction of oriented crystals after programming the temporary shape, whereby a nearly isotropic nanostructure was observed in X-ray scattering experiments. With increasing PCL wt% in CLEG, an increasing orientation of the crystalline phase was obtained and R_f increased up to 100%. This observation was supported by the SAXS measurements and will be discussed later.

The recovery processes are shown in **Fig. 4**. In **Fig. 4a** the actual bending (θ) angle is presented as function of temperature, which was increased in steps of 5 K. Here we obtained five data points per sample as consequence of the experimental setup (single photographs at each temperature) and the lines connecting data are guides for the eyes. The error bars correspond to an experimental error of ±5° (in θ). A complete recovery of the permanent shape was observed (R_r =100%) for bending experiments, where the recovered angle θ_f was 0° for all samples after completing the process. Lower R_r – values were obtained in uniaxial stretching experiments, which we attribute to the applied pre-force during the uniaxial tensile test. The stress-free conditions during the bending recovery allowed the sample to recover completely.

Table 2 Dual-shape properties of CLEG polymer network determined by bending experiment in water.

	Bending experiment		Elongation experiment		
Sample ID [a]	R_f [b] [%]	R_r [b] [%]	R_f [b] [%]	R_r [b] [%]	T_{sw} [c] [°C]
CLEG30	42±2	100±2	33±1	48±2	47±1
CLEG40	59±2	100±2	67±2	50±2	46±1
CLEG50	79±2	100±2	87±2	59±2	46±1
CLEG60	100±2	100±2	100±2	62±2	47±1
CLEG70	100±2	100±2	100±2	70±2	47±1

[a] Sample ID the two-digit number gives the weight content of PCLDIMA in wt% in the starting reaction mixture. [b] Shape fixity ratio (R_f) and shape recovery ratio (R_r) as determined from SMCP and recovery. [c] Switching temperature as determined from the derivative's maximum of the recovery curve.

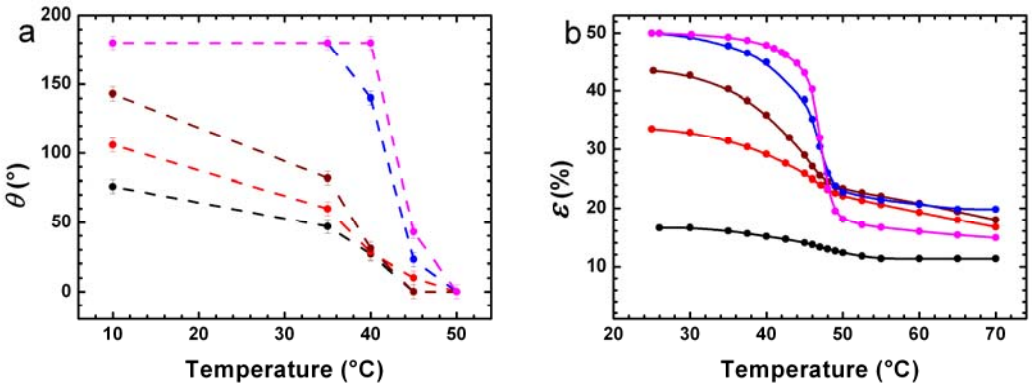

Figure 4: Shape recovery curves under aqueous environment of: CLEG30 (black), CLEG40 (red), CLEG50 (brown), CLEG60 (blue), and CLEG70 (magenta). (a) Recovered angle versus temperature obtained in bending

experiments (from fixed θ_t to recovered θ_f). (b) recovered strain versus temperature plot (from fixed ε_u to recovered ε_p).

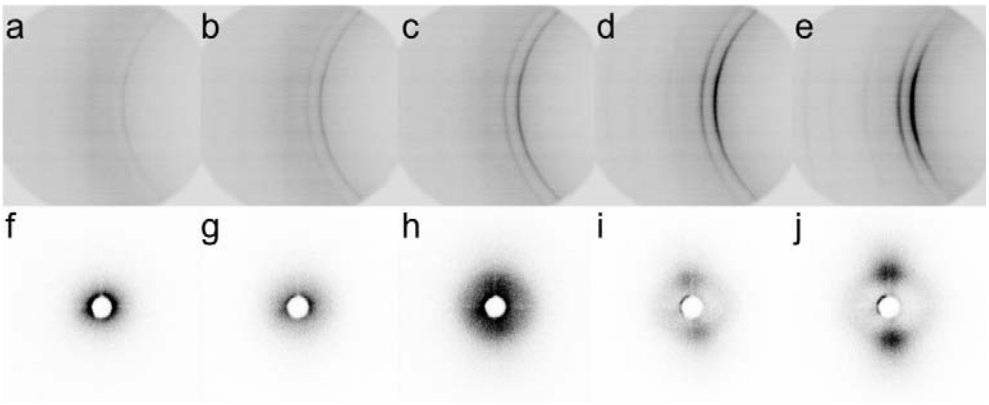

Figure 5: WAXS (a-e) and SAXS (f-j) of CLEG hydrogels under aqueous environment after programming of temporary shape (elongated to ε_m = 40% at T_{high} and cooled to T_{low} under constant strain): CLEG30 (a and f), CLEG40 (b and g), CLEG50 (c and h), CLEG60 (d and i) and CLEG70 (e and j).

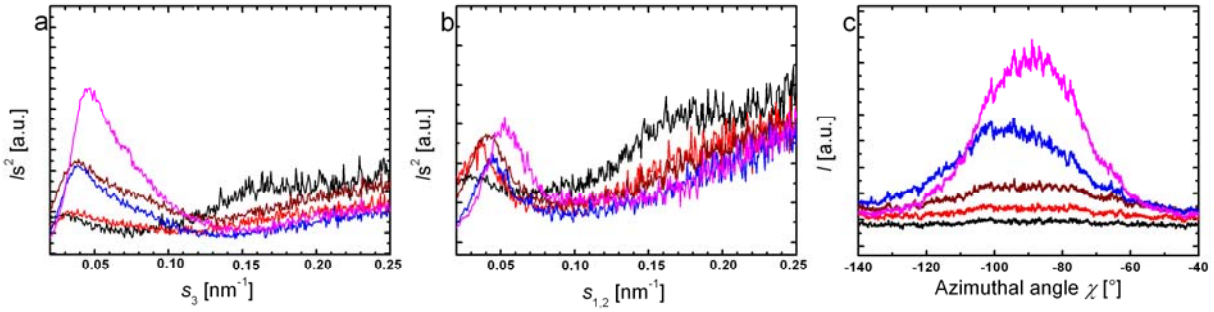

Figure 6: Scattering curves as obtained from SAXS/WAXS of CLEG under aqueous environment after the programming step: (a) SAXS intensity parallel and (b) perpendicular to the drawing direction. (c) Azimuthal intensity profiles for CLEG as obtained from WAXS. CLEG30 (black), CLEG40 (red), CLEG50 (brown), CLEG60 (blue), and CLEG70 (magenta).

The T_{sw}, where the sample attained the most intensive shape change, were determined as inflection points from the strain-temperature recovery curves shown in **Figure 4b**. T_{sw} for all CLEG hydrogels was observed at 46 ± 1 °C, whereby the switching temperature interval (ΔT_{rec}) was found to decrease with increasing PCL content. We attributed the decreasing of ΔT_{rec} to an increased lateral crystal size of CLEG with higher semi-crystalline PCL fraction after the programming step as larger crystals melted closer to $T_{m,PCL}$.

3.4. Structural investigations by SAXS/WAXS

The strongest (hk0) reflections present in the WAXS-patterns of the CLEG in aqueous environment were the (110) located at 2θ = 21.3° and the (200) at 23.8°. The peak position and therefore the dimensions of the unit cell did not change for different CLEG compositions

or dual-shape programming stages. The non-programmed/original swollen CLEG was always isotropic, having the crystalline domains distributed randomly in space. Thus an azimuthal integration over a desired reflection (e.g. (110)) leads into flat curves I versus χ. As CLEG30 did not reach 50% elongation during the programming step, we have chosen the maximum common elongation ε_m for all samples, which was 40% (because single CLEG30 specimens reached 40%). Therefore the structural information of all CLEG hydrogels is comparable within the series regarding crystallinity and orientation. Once the CLEG was programmed, after 40% elongation at T_{high} and fixing the temporary shape by cooling to T_{low}, scattering patterns as exhibited in **Fig. 5a-e** were obtained from samples swollen to equilibrium. On one hand the increasing intensity of the crystalline reflections was observed with increasing PCL wt%, being analogous to the isotropic precursors, resulting from the increased crystallinity (shown in Ref. [18]). On the other hand, we observed an increased degree of orientation with increasing PCL wt% as reflected by the increased sharpness of the χ profile of the (110) and (200) reflections.

The WAXS-patterns were taken from the equatorial section of the full pattern, being the drawing direction vertical, and finding the (110) and (200) diffraction peaks on the equator. This was attributed to the orientation of the crystal c-axis parallel to the direction of the deformation as the a- and b-axis were perpendicular as observed by equatorial (hk0) reflections. Here the character of the PCL as the backbone of the polymer network became evident. Upon deformation during the dual-shape programming, the PCL chains and thus the c-axis of the crystallizable fixing domains were aligned parallel to the stretching direction. A reflection having information along the c-axis (e.g. a (002) reflection) could not be observed and thus crystalline extension along the direction of deformation (fiber axis) could not be discussed from WAXS.

The average crystal size was estimated using the Scherrer equation as described in the experimental section for both the (110) and (200) reflections (c.f. **Table 3**). Isotropic CLEG, i.e. before the programming was applied, had an increased crystal size with increasing PCL content ranging from 13 nm normal to the (110) plane for CLEG30 to 15 nm for CLEG70. The crystal size normal to the (200) plane increased from 9 nm for CLEG30 to 12 nm for CLEG70. This was attributed to the larger PCL-populated regions with increased PCL wt%, which allowed the growth of larger crystals. CLEG30 and CLEG40, having the highest wt% of PEG side chains, which are grafted to the backbone and surrounded by primary bound water, inhibited the formation of larger PCL crystallites.

Table 3 Crystal sizes as determined from the (110) at 21.3° and (200) at 23.8° reflections of the WAXS patterns of CLEG prior and after programming and long-periods parallel and perpendicular to the programming axis.

	Crystal sizes				Domain correlation	
	$\varepsilon = 0$ %		$\varepsilon = 40$ %		$\varepsilon = 40$ %	
Sample ID [a]	l_c **(110)** [b] **[nm]**	l_c **(200)** [b] **[nm]**	l_c **(110)** [b] **[nm]**	l_c **(200)** [b] **[nm]**	$L(s_3)$ [c] **[nm]**	$L(s_{1,2})$ [c] **[nm]**
CLEG30	13.1±0.5	8.6±0.5	11.9±0.5	8.4±0.5	30.9±0.5	33.2±0.5
CLEG40	15.2±0.5	9.7±0.5	11.9±0.5	7.3±0.5	27.1±0.5	27.4±0.5
CLEG50	14.5±0.5	11.2±0.5	12.4±0.5	8.2±0.5	26.7±0.5	24.3±0.5
CLEG60	15.4±0.5	11.1±0.5	14.2±0.5	10.9±0.5	26.0±0.5	22.8±0.5
CLEG70	14.9±0.5	12.5±0.5	14.3±0.5	10.2±0.5	22.0±0.5	19.1±0.5

[a] Sample ID the two-digit number gives the weight content of PCLDIMA in wt% in the starting reaction mixture. [b] Crystal sizes as determined from the (110) and (200) diffraction of CLEG under aqueous environment. [c] Long periods of CLEG under aqueous environment determined parallel (s_3) and perpendicular ($s_{1,2}$) to the drawing direction.

After SMCP the crystal sizes were extracted from the equatorial section of the WAXS-pattern, increasing from 12 to 14 nm (110) and from 8 to 10 nm (200) for CLEG30 to CLEG70 respectively (**Table 3**). Here the slightly decreased size as compared to the isotropic samples was attributed to homogenization of the co-polymer structure after alignment. Whereas isotropic samples had more degrees of freedom to allow phase separation between hydrophobic PCL and hydrophilic PEG, upon deformation and alignment of the polymer network the phase separation was reigned by the molecular structure (i.e. the positions of the grafted PEG chains) and the formation of hydrophobic PCL domains was slightly hindered, resulting in decreased crystal sizes after SMCP as compared to non-programmed samples.

The arrangement of the crystalline domains was investigated by SAXS of CLEG hydrogels after SMCP under aqueous environment. Scattering patterns are shown in **Fig. 5f-j**. As a first observation, the scattering intensity increased with the PCL wt% and was lowest for CLEG30 and CLEG40 (analogous to the WAXS-pattern). Above 50 wt% of PCL, the scattering patterns became clearly anisotropic, exhibiting two distinct point-like reflections located on the meridian and having a ring-like signal with lower intensity. This was related to lamellar like crystals having correlation in the stretching direction (point reflections on the meridian) and a smaller fraction of un-oriented crystals (ring reflection).

The anisotropic SAXS patterns were evaluated in two directions as described in the experimental part, parallel to the drawing direction (where the point-like reflections were located) and perpendicular to the stretching in order to investigate the correlation on the crystalline domains in two directions. The Lorentz corrected scattering curves are presented in

Fig. 6 for both directions, allowing the extraction of the long-period (including one crystalline and one amorphous domain) parallel and perpendicular to the direction of deformation. We observed an increased intensity of the correlation along the fiber axis with increasing PCL content (**Fig. 6a**), as reflected by the increased intensity of the peak and attributed to the increased number of semi-crystalline PCL domains contributing to the scattering intensity. We also observed a remnant correlation perpendicular to the drawing with a slightly increased intensity with increasing PCL wt% (**Fig. 6b**).

The long periods as extracted from the peak positions are shown in **Table 3**, exhibiting a decrease from 31 to 22 nm along the fiber axis for CLEG30 to CLEG70 respectively, which was attributed to increased crystallizable PCL fraction leading into smaller average distances between crystals. The remnant lateral correlation (perpendicular to the drawing) decreased from 33 to 19 nm with increasing PCL wt%. Long periods were similar in both directions for CLEG30 and CLEG40 (around 31 and 27 nm respectively) and had a difference for CLEG50, CLEG60, and CLEG70 as observed in **Table 3**. This was attributed to the increased orientation and thus rearrangement of the nanostructure upon SMCP (also observed in the WAXS-pattern). The smallest fractions of hydrophobic PCL (in CLEG30 and CLEG40) were relatively distant in the polymer network, after deformation at T_{high} and cooling to T_{low} the crystallized domains showed only weak correlation, thus after removal of the strain constraint (last step of the SMCP) the crystallites could swap back into an energetic favored random state (isotropic). Thus the WAXS-patterns showed flat I versus χ profiles and the correlation of the domains is low (SAXS intensity of the correlation-peaks). Similar observations have been reported for dry CLEG during triple-shape-memory programming [19], where only the PCL main-chain had a clear orientation after SMCP. CLEG having 60 or 70 wt% of PCL had a different nanostructure after SMCP. We observed the increased orientation of the crystalline PCL in the azimuthal WAXS profile and oriented lamellae-like character in the SAXS having dominant longitudinal correlation. After SMCP, once the strain constraint is released, the oriented nanostructure had stability as the oriented crystallites could not swap into isotropic confirmations. This resulted macroscopically into a high ability to fix a temporary shape as reflected by $R_f = 100\%$.

We conclude that the fixing ratio was controlled by the formation of lamellae-like crystals having correlation in the direction of the deformation. These nanostructures appeared at higher PCL content (CLEG60 and CLEG70) and R_f was 100%. The average lateral crystal size, attributed to the lamellae lateral extension, was 14 nm for CLEG60 and CLEG70 (estimated from (110) reflection). Decreasing PCL wt% led into decreased average lateral

crystal size and showed no oriented lamellae-like character in the SAXS-pattern, moreover the correlation between crystalline domains was reduced (lower intensity) and the distance increased (larger long period). This nanostructure resulted into physical netpoints, which had only limited capability to fix a temporary shape, as reflected by R_f lowered to 33%.

4. Conclusions

CLEG with different composition were successfully synthesized by thermally-induced radical polymerization. Swelling of CLEG copolymer networks in water until equilibrium state resulted in hydrogels. The water swelling capability of CLEG was strongly correlated with the content of PEG, whereas overall crystallinity under aqueous conditions was related to the weight content of PCLDIMA crosslinker in the starting reaction mixture. The thermal and mechanical properties as well as the crystallinity of CLEG were found to be reduced by the uptake of water. All CLEG copolymer networks exhibited a pronounced dual-shape effect, exhibiting shape fixity and shape recovery ratios up to 100%. T_{sw} was reduced by the uptake of water from 55 °C (dry networks) to 46 °C. The analysis with SAXS/WAXS exhibited that crystallinity, as well as orientation and size of the crystallized domains control the dual-shape-memory performance. For CLEG hydrogels having >50 wt% of PCL, a degree of crystallinity >14% (ΔH_m = 19 J·g^{-1}) enabled the formation of large lamellae-like structures, which became oriented after SMCP and resulted in R_f = 100%. It can also be anticipated that the presented CLEG polymer systems, which combine dual-shape capability and degradability are promising candidate materials for biomedical applications such as controlled drug release systems [3].

References

1. Behl M, Lendlein A. Actively moving polymers. Soft Matter 2007:3:58-67.
2. Ratna D, Karger-Kocsis J. Recent advances in shape memory polymers and composites: a review. Journal of Materials Science 2008:43(1):254-269.
3. Wischke C, Neffe AT, Steuer S, Lendlein A. Evaluation of a degradable shape-memory polymer network as matrix for controlled drug release. Journal of Controlled Release 2009:138(3):243-250.
4. Wagermaier W, Kratz K, Heuchel M, Lendlein A. Characterization methods for shape-memory polymers. Advances in Polymer Science 2010:226:97-145.
5. Huang WM, Yang B, An L, Li C, Chan YS. Water-driven programmable polyurethane shape memory polymer: Demonstration and mechanism. Applied Physics Letters 2005:86(11):114105.
6. Pierce BF, Bellin K, Behl M, Lendlein A. Demonstrating the influence of water on shape-memory polymer networks based on poly[(rac-lactide)-co-glycolide] segments in vitro. International Journal of Artificial Organs 2011:34(2):172-179.
7. Yang B, Huang WM, Li C, Li L. Effects of moisture on the thermomechanical properties of a polyurethane shape memory polymer. Polymer 2006:47(4):1348-1356.
8. Yu YJ, Hearon K, Wilson TS, Maitland DJ. The effect of moisture absorption on the physical properties of polyurethane shape memory polymer foams. Smart Materials & Structures 2011:20(8):085010.
9. Osada Y, Matsuda A. Shape memory in hydrogels. Nature 1995:376(6537):219-219.
10. Tanaka Y, Kagami Y, Matsuda A, Osada Y. Thermoreversible Transition of Tensile Modulus of Hydrogel with Ordered Aggregates. Macromolecules 1995:28(7):2574-2576.
11. Kagami Y, Gong JP, Osada Y. Shape memory behaviors of crosslinked copolymers containing stearyl acrylate. Macromol Rapid Commun 1996:17(8):539-543.
12. Lin XK, Chen L, Zhao YP, Dong ZZ. Synthesis and characterization of thermoresponsive shape-memory poly(stearyl acrylate-co-acrylamide) hydrogels. Journal of Materials Science 2010:45(10):2703-2707.
13. Xu X, Davis KA, Yang P, Gu X, Henderson JH, Mather PT. Shape Memory RGD-Containing Networks: Synthesis, Characterization, and Application in Cell Culture. Macromolecular Symposia 2011:309-310(1):162-172.
14. Hoffman AS. Hydrogels for biomedical applications. Adv Drug Delivery Rev 2002:43:3-12.
15. Narendra Kumar U, Karl Kratz, Marc Behl and Andreas Lendlein. Triple-Shape Capability of Thermo-sensitive Nanocomposites from Multiphase Polymer Networks and Magnetic Nanoparticles. Mater Res Soc Symp Proc 2009:1190:55-61.
16. Bellin I, Kelch S, Langer R, Lendlein A. Polymeric triple-shape materials. Proceedings of the National Academy of Sciences of the United States of America 2006:103(48):18043-18047.
17. Behl M, Lendlein A. Triple-shape polymers. J Mater Chem 2010:20(17):3335-3345.
18. Kratz K, Narendra Kumar U, Noechel U, Lendlein A. Thermal Properties and Crystallinity of Grafted Copolymer Networks containing a Crystallizable Poly(ε-caprolactone) Crosslinker in an aqueous environment. Mater Res Soc Symp Proc 2012:1403:73-78.
19. Wagermaier W, Zander T, Hofmann D, Kratz K, Narendra Kumar U, Lendlein A. In Situ X-Ray Scattering Studies of Poly(ε-caprolactone) Networks with Grafted Poly(ethylene glycol) Chains to Investigate Structural Changes during Dual- and Triple-Shape Effect. Macromolecular Rapid Communications 2010:31(17):1546-1553.
20. Scherrer P. Bestimmung der Größe und der inneren Struktur von Kolloidteilchen mittels Röntgenstrahlen. Göttinger Nachrichten Math Phys 1918:2:98-100.

21. Stribeck N. X-Ray Scattering of Soft Matter. Heidelberg, New York: Springer, 2007.
22. Mooney M. A Theory of Large Elastic Deformation. J Appl Phys 1940:11(9):582-592.
23. Xia Z, Patchan M, Maranchi J, Elisseeff J, Trexler M. Determination of crosslinking density of hydrogels prepared from microcrystalline cellulose. J Appl Polym Sci 2012:Article first published online: 6 JUN 2012, DOI_2010.1002/APP.38052.
24. Sombatsompop N. Analysis of Cure Characteristics on Cross-Link Density and Type, and Viscoelastic Properties of Natural Rubber. Polym-Plast Technol Eng 1998:37(3):333-349.
25. Back AL. Relation between Gel Content, Plasticity, and Dilute Solution Viscosity of Elastomers. INDUSTRIAL & ENGINEERING CHEMISTRY 1947:39:1339-1343.
26. Tominaga T, Sano KI, Kikuchi J, Mitomo H, Ijiro K, Osada Y. Hydrophilic Double-Network Polymers that Sustain High Mechanical Modulus under 80% Humidity. ACS Macro Letters 2012:1(3):432-434.